

Rationalization of Dye Uptake on Titania Slides for Dye-Sensitized Solar Cells by a Combined Chemometric and Structural Approach

Valentina Gianotti,^[a] Giada Favaro,^[a] Luca Bonandini,^[b, c] Luca Palin,^[a] Gianluca Croce,^[a] Enrico Boccaleri,^[a] Emma Artuso,^[b] Wouter van Beek,^[d] Claudia Barolo,^{*, [b]} and Marco Milanese^{*, [a]}

This work is dedicated to Professor Davide Viterbo on the occasion of his 75th birthday.

A model photosensitizer (D5) for application in dye-sensitized solar cells has been studied by a combination of XRD, theoretical calculations, and spectroscopic/chemometric methods. The conformational stability and flexibility of D5 and molecular interactions between adjacent molecules were characterized to obtain the driving forces that govern D5 uptake and grafting and to infer the most likely arrangement of the molecules on the surface of TiO₂. A spectroscopic/chemometric approach was then used to yield information about the correlations be-

tween three variables that govern the uptake itself: D5 concentration, dispersant (chenodeoxycholic acid; CDCA) concentration, and contact time. The obtained regression model shows that large uptakes can be obtained at high D5 concentrations in the presence of CDCA with a long contact time, or in absence of CDCA if the contact time is short, which suggests how dye uptake and photovoltaic device preparation can be optimized.

Introduction

Photovoltaic (PV) cells based on organic semiconductors and/or organic light harvesters are potentially extremely inexpensive but their efficiency and stability are still limited compared to inorganic crystalline solar cells. Among them, dye-sensitized solar cells (DSC) represent a promising and emerging technology.^[1] These cells mimic the energy conversion mechanism of photosynthesis as light is absorbed by an antenna compound (chlorophyll in photosynthesis, a dye in DSC), then an excited electron is produced and captured by a complex system (photo systems I and II in photosynthesis and nanostructured titanium oxide, tin oxide, and an inorganic electrolyte in DSC), which exploits the energy to obtain valuable products (i.e.,

chemical energy in the form of sugar in photosynthesis and electric current in DSC).

The chemical properties of the cell components must be designed and tuned carefully to optimize the yield of PV cells. Presently, the main issues that still limit their technological applications^[2] are: 1) the achievement of a reasonable conversion efficiency of the DSC modules (10% for opaque, 5–6% for transparent),^[3] 2) maintaining these yields over the time needed for a cell working in real conditions (~20 years), and 3) the achievement of reproducible results (± 3 –5% differences between modules). To fulfill these objectives, a detailed molecular-level knowledge of the DSC components is of paramount importance.


Although a great deal of research has been performed to design more efficient photosensitizers,^[4] only recently have efforts been made to understand,^[5,6] model,^[7–10] and control^[11] the interactions that play a major role in dye uptake. Moreover, the dye loading amount can be tuned by changing the bath solvent,^[5] which has an important effect on the cell efficiency. Literature data highlight the importance of chenodeoxycholic acid (CDCA) as a coadsorbent to control dye aggregation and electron injection^[12] and to improve the performance.^[13] However, a rationalization of the effect of chemical parameters that affect dye uptake, in relation with chemical forces that govern molecular interactions is still lacking. A polyene-diphenylaniline dye (D5) proposed by Hagberg et al.,^[14] has been used in a case study for the rationalization of the uptake conditions in metal-free dyes. This simple molecule^[7,15] can be considered as a model for the widespread class of donor- π -acceptor (D- π -A)

[a] Dr. V. Gianotti, G. Favaro, Dr. L. Palin, Dr. G. Croce, Dr. E. Boccaleri, Dr. M. Milanese
Dipartimento di Scienze e Innovazione Tecnologica
Università del Piemonte Orientale "A. Avogadro"
Viale T. Michel 11, 15121 Alessandria (Italy)
E-mail: marco.milanese@unipmn.it

[b] L. Bonandini, Dr. E. Artuso, Dr. C. Barolo
Dipartimento di Chimica, NIS Interdepartmental Centre
Università di Torino
Via Pietro Giuria 7, 10125 Turin (Italy)
E-mail: claudia.barolo@unito.it

[c] L. Bonandini
DYEPOWER
Viale Castro Pretorio 122, 00185 Rome (Italy)

[d] Dr. W. van Beek
Swiss-Norwegian Beamlines at ESRF
BP 220, Grenoble 38043 (France)

 Supporting Information for this article is available on the WWW under <http://dx.doi.org/10.1002/cssc.201402194>.

dyes. To date, this class holds the efficiency record for metal-free dyes.^[16] In the last decade, various organic functional groups have been combined to generate D- π -A structures. One of the schemes employed most commonly is: an aryl amine group as electron donor, a thiophene unit as the π linker, and a cyanoacrylic acid moiety as the electron acceptor/anchoring group (which are all present in D5).

Structural and crystallographic studies of organic compounds and molecular complexes allow the assessment of the possible intra- and intermolecular interactions, which are of paramount importance for the functionality of the materials under working conditions.^[17–19] Very few structural studies are found in the field of DSC because of the complications of dye crystallography, which are mainly because of the difficulty to obtain suitable single crystals. Ru-based dye compounds^[20] are less difficult to crystallize and represent the majority of the X-ray crystal structures related to DSC, whereas only a few crystal structures of compounds related to D- π -A sensitizers are available in the Cambridge Crystallographic Data Centre (CCDC).^[21] Relevant structures in the database are: 1) a molecule that contains diphenylaminophenyl and carboxylic moieties, that is, D5 without the vinyl thiophene linker,^[22] and 2) two molecules that contain the diphenylaminophenyl moiety and a thiophene linker.^[23] The electronic and molecular surface structure of the functional dye-sensitized interface has also been studied in detail for D5 by a combination of core-level spectroscopy, valence-level spectroscopy, X-ray absorption spectroscopy, and resonant photoemission spectroscopy.^[24]

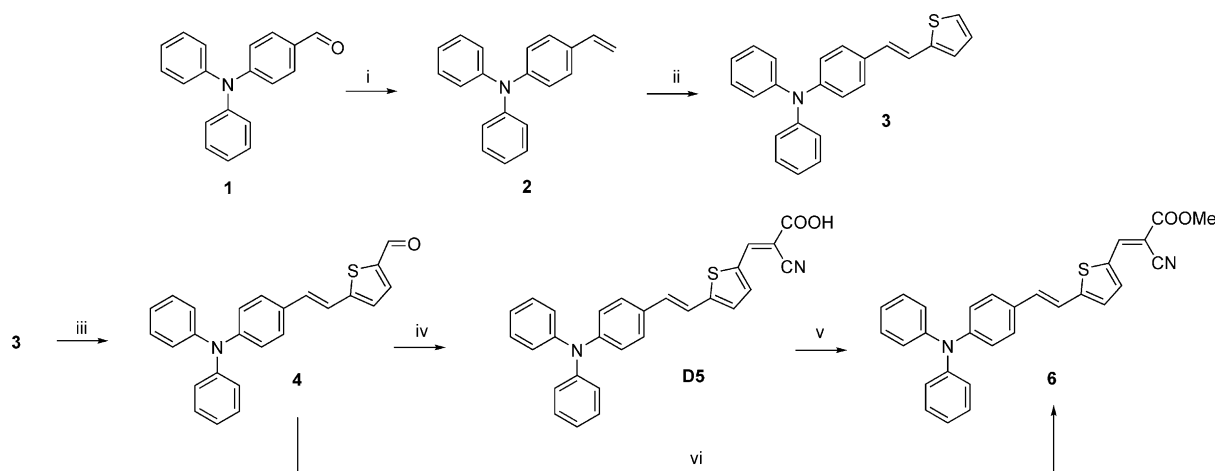
In this study, we intend to shed light on the dye-uptake process by combining design of experiment (DoE) assisted UV/Vis spectroscopy with a structural investigation. Our aim is to understand the mechanism of dye dispersion and bonding to the TiO₂ surface with the long-term goal to understand their influence on the cell macroscopic behavior. In the present study, dye-related crystallography problems have been overcome by exploiting advanced powder XRD methods that use different high-resolution detectors with a high-flux synchrotron-radiation

X-ray source. We report on the crystal and molecular structure of D5 and two related compounds (**4** and **6**; Scheme 1) by powder and single-crystal XRD. The analysis of their packing features allowed us to understand the molecular forces that govern their intra- and intermolecular interactions. However, crystallographic studies cannot give direct information on the behavior of D5 on TiO₂. To shed light on the correlations between the main parameters that govern dye uptake, a chemometric-driven UV/Vis spectroscopic study was designed and performed. UV/Vis spectroscopy was used recently by Dell'Orto et al. to assess the kinetics of the absorption of the N719 dye onto TiO₂.^[11] We chose to exploit a quantitative chemometric approach because it allows the maximization of the information content in the least number of experiments.^[25–27] To date, the optimization of the experimental conditions of dye uptake has been performed mainly by trial and error or at best by “one variable at a time” (OVAT) methods. Only very recently was the chemometric approach proposed in the field of DSC by some of us.^[28] The present work aims to investigate both the molecular structure and the dye uptake in a synergic way and represents the first part of a larger project that we are undertaking with the purpose to understand, at the molecular level, the mechanisms involved in DSC function with the ultimate aim to improve their yields and stability by optimizing the preparation methods of the cell itself.

Results and Discussion

D5 synthesis

The synthesis of **4** and D5 was performed with a slight modification of literature procedures^[14,29] by starting from commercial 4-(*N,N*-diphenylamino)benzaldehyde (**1**; Scheme 1). The first step of our synthetic pathway is a simple Wittig reaction^[30] to obtain alkene **2**, which was used as a substrate for a subsequent Pd-catalyzed decarbonylative Heck reaction^[31] to give intermediate **3**. Subsequently, lithiation of **3** with *n*-butyllithium



Scheme 1. Synthesis of D5 dye. Reagents and conditions: i) Ph₃PCH₃Br, *t*BuOK, THF, RT, 8 h (76%); ii) Thiophene-2-carboxylic acid, PdCl₂, LiCl, di-*tert*-butyl dicarbonate, *g*-picoline, *N*-methylpyrrolidone, 120 °C, 16 h (70%); iii) DMF, BuLi, THF, –78 °C to RT (39%); iv) Cyanoacrylic acid, piperidine, (72%); v) MeOH, H₂SO₄, reflux, 24 h; vi) Cyanoacrylic methyl ester, piperidine, ACN.

followed by the addition of DMF yielded the corresponding aldehyde **4**. The electron-withdrawing group is inserted into the structure by a Knoevenagel reaction between aldehyde **4** and cyanoacetic acid in the presence of piperidine.

D5 was then converted into its corresponding methyl ester (**6**) to verify the configuration of the 2-cyano-3-(thiophen-2-yl) acrylic acid moiety. Compound **6** was also obtained, in the same configuration, through the classical Knoevenagel reaction directly from **4**.

Computational study of D5 conformational flexibility and freedom

The chemical formula of D5 (Figure 1) suggests that this molecule should be rather rigid and planar because of the conjugation between aromatic moieties (thiophene and benzene

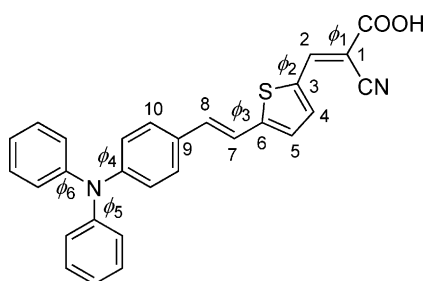


Figure 1. Degrees of freedom of D5 molecule: ϕ_1 , ϕ_2 , and ϕ_3 refer to the O=C1–C2, C1–C2–C3–C4, and C5–C6–C7–C8 torsion angles, respectively.

rings) through a C=C bond. In addition, the cyanoacetic group is planar and connected to the thiophene by a double bond. The only nonrigid part is the 3-phenylamino moiety, which is nonplanar and the terminal phenyl groups are free to rotate and adopt different conformations. The crystal structures of **4** and **6** from single-crystal data gave a clear picture of the stereochemistry around the C=C bond isomerization and confirmed the expected *E* isomer (see below). In addition, NMR spectroscopy and chromatography experiments (Section S1 in the Supporting Information) confirmed that only one isomer is present in solution. Conversely, a rather rich conformational variability can arise because of the rotation around the single bonds, as discussed below. In principle, a reliable indication of the stable conformation of D5 in the solid state could be gained from single-crystal XRD data, but the same indication about the dye in solution or bonded to the TiO₂ surface can only be obtained by a combination of experimental XRD data and computational analysis by first-principles calculations. As we failed in all of our attempts to grow single crystals of D5 because of the well-known difficulty to crystallize bulky carboxylic acids, in analogy to that observed for fatty acids,^[32] high-resolution X-ray powder diffraction (XRPD) was used. The limited resolution of XRPD of organic molecules rendered the discrimination between the isomers rather difficult and, therefore, an accurate conformational analysis was needed.

First-principles calculations on stable minima

In Ref. [9] only one isomer of D5 (named D5-2a in Table 1) is accepted and used generally.^[33] As we lack a single-crystal structure of D5 and as it is almost impossible to investigate the structure of D5 on TiO₂ directly and precisely in solution during the grafting process, accurate first-principles theoretical calculations, combined with an experimental structural study of D5 and its parent compounds, have been performed and reported in detail in a separate paper, together with all the strategies and tricks used for structure solution.^[34]

In this paper, the possible conformational changes were investigated by considering the three degrees of freedom (ϕ_1 , ϕ_2 , and ϕ_3 ; Figure 1), which can assume either the *s-cis* or the *s-trans* conformations as *E/Z* isomerization is already established. The conformational changes around ϕ_4 , ϕ_5 , and ϕ_6 are less important because of the symmetry of the phenyl groups. However, for an exhaustive search they were also considered, but only the more stable conformations of D5 and related compounds are reported (Table S2).

Among the possible theoretical conformers, four of them (namely, D5-1a, D5-1b, D5-2a, and D5-2b) possess stable energy minima below 1.5 kcal mol^{−1}. According to the Boltzmann distribution, they are most probably the dominant ones for D5 in solution and on the TiO₂ surface (i.e., in the relevant cases).

The geometries of the four isomers, after geometric optimization by first-principles calculations at the B3LYP/6-31G(d,p) and B3LYP/6-311+G(2d,2p) levels of theory, are depicted in Table 1. The 6-31G(d,p) basis set was used to obtain a first fast geometry optimization and screening of possible stable conformations, whereas the 6-311+G(2d,2p) basis set was mandatory to obtain a careful description of the molecular geometries of the conformers and of their relative stabilities. Conformer D5-1a is the most stable and also the most prevalent in X-ray crystal structures (see below) and thus can be considered the prevalent structure at equilibrium. The structure reported most commonly (D5-2a)^[14,16] and the other two conformers are less stable by less than 0.5 kcal mol^{−1} and can be present at lower concentrations in solution, according to the Boltzmann distribution, and at nonequilibrium conditions. Notably, if D5 first approaches and is then linked to the TiO₂ surface, the carboxyl group is deprotonated and the conformational degree of freedom around ϕ_1 becomes irrelevant because the COO[−] moiety is symmetric for a 180° rotation. Moreover, in deprotonated D5 the energy differences are even smaller (Table 2).

Therefore, the theoretical calculations suggest that conformers D5-1a, D5-1b, D5-2a, and D5-2b are the most probable. Three out of these four conformations were observed experimentally in the X-ray crystal structures (see discussion below), in which crystal packing forces play a relevant role in the selection of less stable conformers. The compromise between the intrinsic thermodynamic stability of the isolated conformers and the effect of intermolecular interactions in the solid-state is well known and is observed if theoretical calculations are compared with X-ray structures.^[35] Of course, these conclusions

Table 1. Geometric features of the most stable conformers (within 1.5 kcal mol⁻¹) after geometric optimization using B3LYP functional.

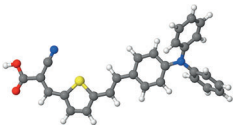
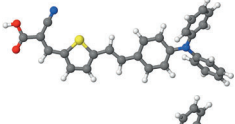
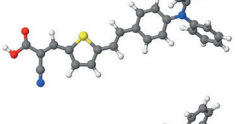
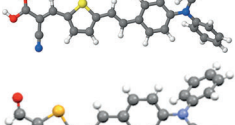
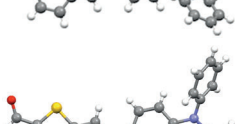
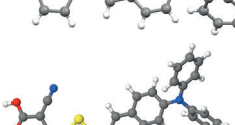
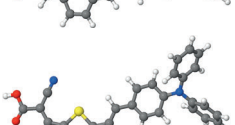
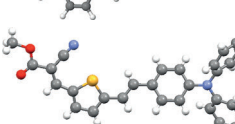
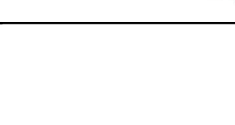
Conformer	ϕ_1 [°]	ϕ_2 [°]	ϕ_3 [°]	Relative stability [kcal mol ⁻¹]		Molecular structure
				6-31G(d,p)	6-311 + G(2d,2p)	
D5-1 a	0.1	180	180	0.00	0.00	
D5-1 b	0.0	180	-1.1	0.95	0.73	
D5-2 a	0.0	0.1	180	0.38	0.34	
D5-2 b	0.0	0.1	-1.8	1.29	0.98	
4	—	-178	-177			
	—	-179	4.7			
D5	-9.3	-173	-169			
	0.6	-168	-175			
6	-0.9	179	166			

Table 2. Relative stabilities after geometric optimization of the more stable conformers for the four models employed in the theoretical calculations.

Model	Relative stabilities [kcal mol ⁻¹]					
	4		deprotonated D5 ⁻		6	
	6-31G(d,p)	6-311 + G(2d,2p)	6-31G(d,p)	6-311 + G(2d,2p)	6-31G(d,p)	6-311 + G(2d,2p)
D5-1 a	0.00	0.00	0.00	0.00	0.00	0.00
D5-1 b	0.98	0.75	1.24	1.11	0.97	0.77
D5-2 a	1.55	1.41	-0.59	-0.51	0.36	0.31
D5-2 b	2.46	2.05	0.79	0.66	1.28	0.99

do not take into account the energy barriers for rotation around the C–C bonds, the investigation of which is discussed in the next paragraph.

their crystal structures. This conformational flexibility is probably important in driving the D5 uptake on TiO₂ as well as the final arrangement of D5 molecules on its surface. The absolute

Energy barriers between energy minima as a function of torsion angles

The rotation barriers between the four conformers were explored by relaxed potential energy scans (R-PES) around the two S–C–C=C torsion angles (ϕ_2 and ϕ_3). To explore this energy surface with an acceptable computing time, initially two 1D R-PES scans were performed at the same DFT level (B3LYP/6-31G(d,p)), and the data are reported in Figure 2a. Then a 2D R-PES at the less-demanding HF/3-21G level of calculation was performed to explore the two torsions, which produced the 3D plot shown in Figure 2b. The basis sets used for geometry optimizations would be too time-consuming and unaffordable for such an extended PES. However HF-3-21G still gave acceptable geometries and energy differences if the energy minima are compared to the results of the more extended basis sets.

The observed minima confirmed that the *s-cis* conformation of D5-1 a is favored and that the other three conformers (D5-1 b, D5-2 a, D5-2 b) are the unique stable minima, in agreement with the first-principles DFT calculations. The R-PES indicated that rotation around ϕ_2 is easier than that around ϕ_3 . Moreover there are no other minima and there are no sterically forbidden regions that hinder the rotation. The heights of the barrier (≈ 4 and 10 kcal mol⁻¹ around ϕ_2 and ϕ_3) suggest that during D5 manipulation, for both the DoE-assisted uptake experiment used here and, in general, for DSC cell preparation, rotation around this single bond is possible, which is also indicated by the fact that **4**, D5, and **6** show different conformations in

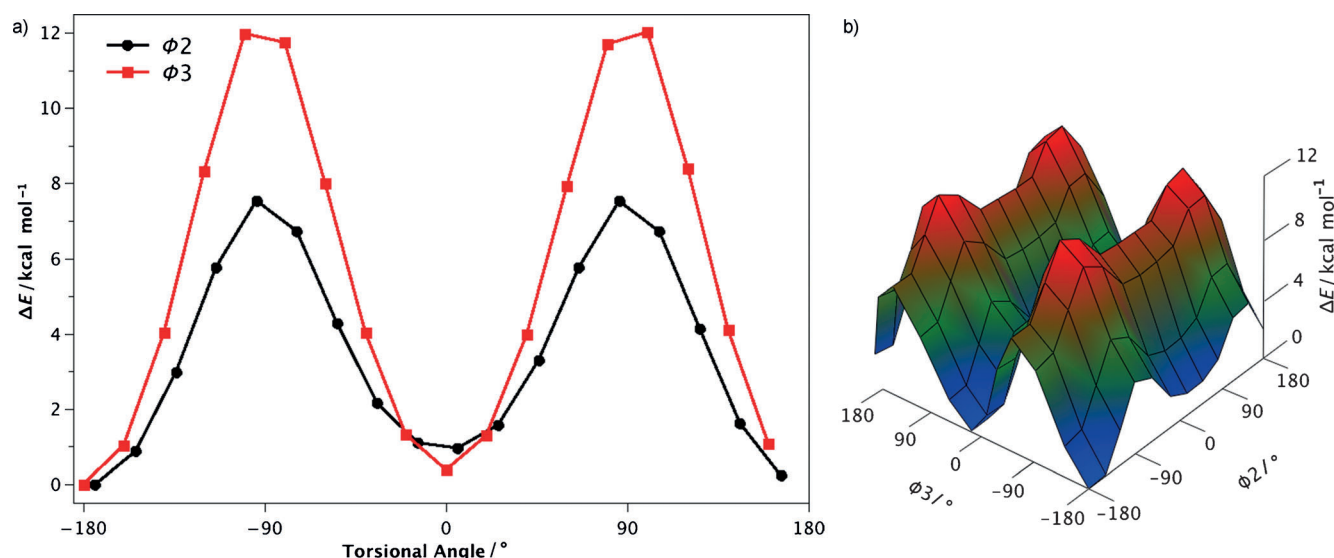


Figure 2. a) Energy profiles for rotation around ϕ_2 (black) and ϕ_3 (red) from B3LYP/6-31G(d,p) calculations, all geometries were fully optimized except for the imposed values of the ϕ_2 and ϕ_3 torsion angles; b) 3D plot of energies obtained from the 2D R-PES.

minimum of the calculations (conformer 1) shows *s-trans* conformation for both ϕ_2 and ϕ_3 torsion angles, whereas the conformation usually considered in the literature (conformer 2) shows *s-cis* and *s-trans* conformations for ϕ_2 and ϕ_3 , respectively. Both conformations are very close in energy and, therefore, accessible at room temperature. The higher stability of the *s-cis* conformation suggested by first-principles calculations was confirmed by looking at the distribution of *s-cis* and *s-trans* conformations in structures containing the vinyl thiophenic moiety in the CCDC database.^[21] This search (Figure S4) confirmed the prevalence of the *s-trans* conformation.

Crystal structures of D5, its precursor 4, and its methyl ester 6

The conformational flexibility suggested by first-principles calculations was confirmed by experimental crystallographic data of **4** and **6**. Despite many different attempts, it was not possible to grow a single crystal of D5 and, as explained before, its structure was investigated by high-resolution synchrotron-radiation XRPD.^[36] The XRPD study was performed under ambient conditions as an experiment at 100 K (at which better data could be collected in principle) a new phase appeared with the formation of a mixture that was impossible to index. For consistency, the data of compounds **4** and **6** were also measured at room temperature. As a result of the well-known limitations of the accuracy of the structures solved by XRPD data, the identification of the correct conformations around the ϕ_1 , ϕ_2 , and ϕ_3 torsion angles without a priori information is a difficult or even impossible task. The conformations depicted in Figure 1 have very small electron-density differences. Even the high-quality data recorded with the 1D analyzer detector (BM1B) and the 2D MAR Image Plate (BM1A) at the Swiss-Norwegian Beamline (SNBL) were not sufficient for a successful structure solution as detailed elsewhere.^[34] To overcome the

problem, on one hand, high-resolution XRPD of excellent spatial and reciprocal space resolution were collected by using a Pilatus 2M detector and, on the other hand, data from theoretical calculations and a priori information from the single-crystal structures of **4** and **6** were exploited. The crystallization of these two parent compounds was straightforward, and their single-crystal structures could give direct and accurate indications about the more stable conformation in the solid state. Notably, both structures **4** and **6** showed that the most stable conformations coincide with those of first-principles calculations. This information helped the interpretation of the XRPD from D5. Initially, the single-crystal structure of **4** was solved to determine the torsion angle ϕ_3 and the common geometric features of these compounds, that is, the planarity of the thiophene group and the geometry of the diphenylamino chromophore. Then **6** (a crystalline derivative of D5) was prepared to obtain experimental data from single-crystal XRD data to shed light on the conformational features of the 2-cyanoacrylic moiety, that is, on the conformation around the ϕ_1 and ϕ_2 torsion angles. In the following sections the relevant features of the three structures are discussed, and crystal data are reported in the Supporting Information.

Single-crystal structures of 4 and 6

Compound **4** crystallizes in the $P\bar{1}$ space group, and the asymmetric unit contains two molecules arranged in parallel along their elongation axis in which one is rotated by $\approx 90^\circ$ with respect to the other to form T-shaped interactions between the aromatic conjugated moieties (Figure 3). The two molecules show two different conformations (*s-cis*, *s-trans*) for the ϕ_3 torsion angle (Table 1), which confirms the possibility that there is more than one stable conformation as suggested by theoretical calculations. Conversely, ϕ_2 shows an *s-trans* conformation

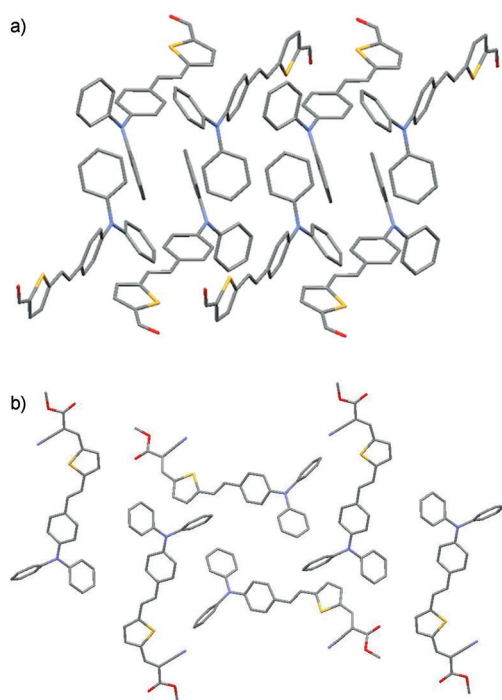


Figure 3. Crystal packing of a) **4** and b) **6** that highlight the hydrophobic clustering of the phenyl groups in both cases.

in both molecules. A short S...O intramolecular contact ($d_{\text{mean}} = 3.04(8)$ Å) is observed.

With regard to the triphenylamine group, the N atom is very close to sp^2 hybridization as the three C–N–C angles are between 118 and 122° and the torsion angle that defines the pyramidity of N (i.e., that obtained by the N atom and the three C atoms bonded to the N atom) is very close to 0°, as expected for a perfect sp^2 hybridization. The two terminal phenyl groups are not coplanar to minimize their reciprocal steric hindrance. The remaining part of the molecule is planar with deviations smaller than 4° in all torsion angles and ϕ_1 and ϕ_2 . Finally, hydrophobic inter- and intramolecular interactions between the phenyl groups of the dibenzylaminic moieties are present.

Compound **6** crystallizes in the $P2_1/c$ space group with one molecule in the asymmetric unit. The triphenylamine and thiophene moieties have geometries similar to those of **4**, and the cyanoacetic group is coplanar to the rest of the molecule. The most relevant information is given by the conformational arrangement around ϕ_2 and ϕ_3 , which are both close to 180° with a *s-trans* conformation within 6° (Table 1) as in the absolute minimum of the first-principles calculations. A short S...N intramolecular contact ($d = 3.26(7)$ Å) is observed. The crystal packing of **6** is driven exclusively by short-contact interactions (less than the sum of the van der Waals radii) because no H bonding is possible. Hydrophobic interactions between the phenyl moieties are observed, similar to those in **4**. Furthermore, the molecular packing reveals that the short-contact network is formed by the intermolecular interaction between the triphenylamine and cyanoacetic groups of adjacent molecules.

Structure of D5 from XRPD data

The unit cell of D5 can contain four molecules and, given the $P\bar{1}$ symmetry with only the inversion center as the symmetry element, two molecules must be present in the asymmetric unit. To solve the structure without biasing the search and to explore the structure solution hypersurface under the best conditions, all four stable isomers D5-1a, D5-1b, D5-2a, and D5-2b were used as starting points for the real space structure solution of D5, and two molecules with different conformations were also combined as observed for **4**. If the simulated annealing searches are extended sufficiently, in terms of temperature and time, the results converged to a solution with ϕ_2 close to 0°, and acceptable solutions were obtained with ϕ_3 close to both 0° and 180°. In other words, two possible correct structure solutions are suggested by simulated annealing. The first has two molecules with the conformation D5-1a and small differences in the planarity of the vinyl thiophene moiety and in the arrangement of the three phenylamino groups, and the second has two different conformations, D5-1a and D5-1b, as observed for **4**. Conformations D5-2a and D5-2b do not appear in any possible stable solutions among the *R* values ranked highly. The best fit of the XRPD data (Figure S3) was obtained for the first arrangement with two D5-1a molecules (the absolute minimum of the first-principles calculations) in the asymmetric unit (Table 1).

The packing driving forces are head-to-tail H bonds between the COOH moieties of adjacent D5 molecules (Figure 4). Hydro-

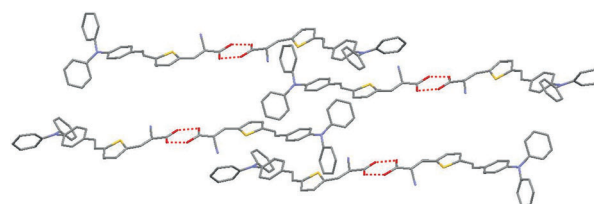


Figure 4. Crystal packing of D5 that shows H bonds and hydrophobic interactions between aromatic groups.

phobic clustering of phenyl groups is observed as in **4** and **6**. It can be concluded that the phenyl–phenyl interactions are the common feature of all three solved crystal structures and must be important also if D5 is bound to TiO₂ nanoparticles. Apart from these common features, it is surprising that the crystal packing of D5 and its precursor are different. Although parallel π – π stacking interactions are observed in D5, in **4** the molecules are pillared perpendicularly with T-shaped interactions (Table S4). Compound **6** shows a completely different packing without stacking of the planar aromatic moieties, but the phenyl–phenyl interactions are still observed. The torsion angles ϕ_2 and ϕ_3 are almost planar (Table 1) but with deviations, within 10°, larger than those suggested by theoretical calculations (in which deviations from 0 and 180° are within 2°; Table S4). Such freedom is confirmed by calculated PES, and a rather flat energy trend is observed between –20 and +20° and –160 and +160° (Figure 2a), and by experimental

data in the literature (Figure S4). The variety and richness of the molecular interactions and deviation from planarity highlighted by crystallographic and computational studies, which probably also occurs also in solution and after adsorption on the TiO_2 surface, suggest that dye uptake is a complex phenomenon that requires a quantitative study for optimization in both material use and cell performance.

Chemometric study of D5 uptake

A full factorial design (FFD) was used that took into account all the parameters involved in the dye uptake to maximize the information with the minimum number of experiments performed.^[37] A DoE approach allows us to evaluate the effect of three variables on two series of samples (TiO_2 powder and slides) in triplicate by performing only 22 experiments. If we used a standard 3D experimental grid, 162 experiments ($3^3 \times 3 \times 2$) would be necessary.

Preliminary experiments with P25 powder were performed to estimate the correct range of D5 concentrations for the uptake study. Then a first FFD was performed using different amounts of P25 powder put in contact with D5 solutions at different concentrations with and without the presence of a dispersant (CDCA) to evaluate the effects of these parameters in a model system. Finally, an FFD experiment applied to a more complex and realistic model on standard TiO_2 slides was performed to explore the mutual influence of three parameters (D5 concentration, CDCA concentration, and soaking time (t)) on D5 uptake in real systems.

A simple, fast, and nondestructive method for dye-uptake evaluation is UV/Vis spectroscopy, which can measure indirectly but precisely the amount of dye extracted from solution by both TiO_2 powders and slides.^[38,39] The direct evaluation of the amount of grafted dye can be undertaken by disruptive and more time-consuming methods such as UV/Vis spectroscopy after dye desorption (with the implicit risk of partial degradation of the dye) or thermogravimetric analysis (TGA; which is less selective and precise and has the drawback of that it is not applicable to standard electrodes) on powdered TiO_2 samples. For these reasons, the indirect UV/Vis method was selected for extensive FFD studies on real samples, and TGA measurements were used to validate some relevant uptake conditions on P25 powders.

Preliminary evaluations

UV/Vis spectra of D5 ethanol solutions at different concentrations were measured to obtain a mean value of the molar extinction coefficient (ϵ) of $35\,530\text{ cm}^{-1}$ at $\lambda = 448\text{ nm}$ as the only reported value was measured in acetonitrile.^[15] Notably, the maximum number of D5 molecules that can be grafted theoretically must not exceed the physical sorption limit. To stay below this limit, suitable amounts of D5 and P25 for the adsorption should range from $1.0\text{--}5.0 \times 10^{-4}\text{ M}$ in 10 mL of D5 solution if amounts of P25 of 1.0–5.0 mg are used. The indirect evaluation of dye uptake by UV/Vis measurements requires that the process consumes a significant mole fraction of dye

(not less than $\approx 0.1\%$, as estimated from molar extinction coefficient and the concentration of D5). To find the correct ranges of D5 concentrations and P25 amounts, we assumed the chemical formula of TiO_2 (anatase phase, density 4.23 g cm^{-3}), a spherical shape of the particles with an average diameter of $\approx 20\text{--}25\text{ nm}$ (confirmed by Scherrer particle size analysis from grazing-incidence XRPD data collected from TiO_2 -covered slides; Figure S1), the weight of one sphere of P25 is $3.1906 \times 10^{-17}\text{ g}$, and the surface available for the sorption per mg of P25 is $6.14 \times 10^{16}\text{ nm}^2$. Moreover, as evaluated with MOLDRAW,^[40] a molecule of D5 bound to the sphere by the cyanoacetic group in which the diphenyl amino moiety forms the outer part covers approximately 0.5 nm^2 .

The results obtained from these preliminary uptake experiments are reported in Table 3. In each experiment, P25 was put in contact with the D5 solution for 16 h at 25°C in a dark

Table 3. D5 uptake on P25 powders.

Experiment	D5 concentration [mmol L ⁻¹]	Amount of P25 [mg]
1	0.1	1.0
2	0.5	1.0
3	0.1	5.0
4	0.5	5.0
5	0.3	2.5
6	0.3	2.5
7	0.3	2.5

bottle to protect the solution from the light. The results are expressed as the number of D5 molecules (molec) retained under batch conditions by 1.0 mg of P25 [molec mg^{-1}]. In the planned experiments, the maximum and minimum levels of the variation ranges of D5 and P25 (experiments 1–4) were selected; moreover, to evaluate the experimental error associated with the method, three replicates were performed with both variables fixed to the values that correspond to the center of the ranges (experiments 5–7). The evaluated standard deviation associated with the methodology was $4.77 \times 10^{16}\text{ molec mg}^{-1}$, and the measured differences in the quantity of grafted D5 are, therefore, statistically significant.

The obtained data confirmed that the sorption is affected by both variables with a positive correlation (the amount of grafted D5 increases as the amounts of both D5 and P25 increase) and allowed us to optimize the experimental procedure.^[41] Notably, the recorded UV/Vis spectra of the concentrated D5 solutions show that the wavelength of the absorption maximum has a bathochromic shift of $\approx 20\text{ nm}$, which is probably caused by the attractive intermolecular interactions highlighted by XRD analysis that are more likely to occur in concentrated solutions. To avoid these aggregation processes, the dispersant CDCA must be included in the real uptake experiments on TiO_2 powders and slides.

D5 sorption on P25 powder

2³ FFD

P25 powder was used as the simplest possible model system. A FFD was planned to investigate the effect of D5 concentration, contact time (t), and CDCA concentration.^[7] To investigate the principal and the interaction effects of the three variables, an FFD 2³ plan was performed, and the eight required experiments (experiments 1–8) are reported in Table 4; moreover,

Table 4. Experimental data from 2³ FFD on TiO₂ powders. + and – represent the highest and the lowest values of the variables.

Experiment	D5	t	CDCA	D5 conc. [mmol L ⁻¹]	t [h]	CDCA conc. [mmol L ⁻¹]	D5 uptake [10 ¹⁶ molec mg ⁻¹]
1	–	–	–	0.04	4.0	0.0	8.1
2	+	–	–	0.40	4.0	0.0	8.4
3	–	+	–	0.04	28.0	0.0	7.3
4	+	+	–	0.40	28.0	0.0	13.5
5	–	–	+	0.04	4.0	16.0	5.7
6	+	–	+	0.40	4.0	16.0	5.2
7	–	+	+	0.04	28.0	16.0	4.4
8	+	+	+	0.40	28.0	16.0	12.0
9	0	0	0	0.22	16.0	8.0	8.0
10	0	0	0	0.22	16.0	8.0	8.2
11	0	0	0	0.22	16.0	8.0	8.2

three replicates of the central experiment (experiments 9–11) were performed at the beginning, in the middle, and at the end of the FFD to confirm the repeatability and to estimate the experimental error.

The results reported in Table 4 were used to calculate an ordinary least-squares (OLS) regression model that relates the experimental result y , that is, the amount of grafted D5, to the experimental factors (D5 and CDCA concentrations and contact time) and their interactions. The significant effects were evaluated by Student's t test in which each regression coefficient was compared with the standard error multiplied by the appropriate Student's t value of 2.92 ($\alpha=95\%$, three degrees of freedom).

The following OLS model was obtained for D5 uptake by powdered TiO₂ [10¹⁶ molec mg⁻¹], that is, Y_p in Equation (1):

$$Y_p = 8.11 + 1.69 \text{ D5} + 1.24 t - 1.25 \text{ CDCA} + 1.73 \text{ D5 } t \quad (1)$$

This is satisfactory as the R^2 value is 0.9914 and the observed and predicted values are in good agreement (Figure S5 A).

The OLS model indicates the relevant factors and their effects on the amount of adsorbed D5. The higher the value of the coefficient in each term, the more important the effect of the factor on the response. + or – indicate an increase or decrease of the D5 uptake if the considered factor is increased. All the principal factors are relevant from statistical analysis of experimental data: the concentration of D5 and t are both associated with a positive effect, whereas the concentration of CDCA has a negative effect, that is, high CDCA concentrations

hamper high uptakes. Nevertheless, for the comprehension of the system, the effects of the interaction of the factors, if relevant, must be considered. The interaction of the factors allows us to describe the simultaneous effects that the factors exert on the system in either a synergic or antagonistic way. In our case, only the interaction between the concentration of D5 and t is relevant; a graphical method based on a two-way table is the best approach to highlight their mutual interaction.

Two-way Table 5 was built by averaging the response of each couple of combinations with the same values of the two

Table 5. Two-way table that illustrates the D5* t two-factor interaction.

D5 uptake [10 ¹⁶ molec mg ⁻¹]		
D5 concentration [mmol L ⁻¹]	0.40	12.7
	0.04	5.9
		4.0
		28.0
		t [h]

variables: the D5 concentration values are the rows and the t values are the columns, so the bottom left quadrant represents the experiments characterized by the lowest D5 value (–) and the lowest t value (–); as there are two experiments with these values (experiments 1 and 5) the average of the responses given by two experiments is reported in the table.

In the bold central cell, on moving from left to right, the D5 concentration is kept constant (and t goes from the lowest to the highest value), conversely, on moving from bottom to top, t remains constant and the D5 concentration increases.

On one hand, D5 and t show a synergic effect as the largest values of dye uptake were obtained, as expected, if high concentrations of D5 were put in contact for a long time (top right corner). Under these conditions, the synergistic effect is dominant with respect to the CDCA concentration as no relevant variations in the amount of dye uptake were recorded in the experiments with or without the dispersing agent (experiments 4 and 8 in Table 4). On the other hand, both intermediate conditions (long soaking time and low D5 concentration or short soaking time and high D5 concentration) reduce D5 uptake with respect to low D5 concentration and short t (bottom left corner).

In these experiments the result of the F test^[42] for the presence of the quadratic effect was negative, so additional experiments to evaluate further variable levels, besides the three chosen ones, would not add any new information about the studied system.

The adopted method can measure precisely but indirectly the amount of dye extracted from the solution by TiO₂ powders and slides. The method was validated by evaluating the quantity of grafted dye by TGA measurements, which have the advantage of directly detecting the amounts taken up but have the drawback that they are less precise and not applicable to slides used in technological applications.

Thermogravimetric analysis

TGA was performed in air on D5, CDCA, and pure TiO₂ powder as reference materials (Figure S6A) and on D5-sensitized TiO₂ powders with and without CDCA under the same conditions of experiments 4 (+ + −) and 6 (+ − +) (Table 2), which correspond to the highest uptake in the absence and presence of CDCA, respectively (Figure S6B). Full TGA data plots and comments are available in the Supporting Information. UV/Vis spectroscopic indirect determination indicated an uptake of 1.0×10^{17} molecules of D5 for 3.0 mg of P25. If we take into account the molecular weight of D5, this corresponds to an expected weight loss of 2.7%. TGA data indicated a weight loss between 3 and 6% for the two analyzed samples, which depended on the adsorption conditions. These values are in agreement with the previous determination (same order of magnitude as the UV/Vis measurements) and confirm that the dye that has left the solution, detected precisely by UV/Vis measurements, was actually grafted on the TiO₂ powder.

The TGA profiles of P25 and D5-sensitized P25 are significantly different (Figure S6). The first consideration, which confirms a chemical interaction between the dye and the substrate, is the clear difference in the thermal degradation profile shown by pure D5 with respect to the D5-sensitized sample. This suggests that the effect of the contact does not originate a physical mixture, but instead, a system with strong interfacial interactions, which is able to modify the thermal degradation profile significantly.

Although pure P25 shows a total weight loss of 1.4%, with a significant contribution caused by the desorption of physisorbed water, the D5-sensitized sample has a lower weight residue because of the decomposition of the organic dye, which leads to a final weight loss of 7.4%.

To quantify the amount of dye in the sample, a weight loss contribution of P25 similar to that of the neat material (1.4%) should be assumed and subtracted from 7.4% to obtain 6.0%. As D5 degrades only for the 95.9% of its initial weight, the neat weight loss caused by D5 can be estimated to be $\approx 6.3\%$ of the total weight of the sample.

The estimated value of adsorbed D5 molecules per gram of P25 from these measurements is 9.0×10^{19} molec g^{−1}. This result is consistent with the indirect UV/Vis measurements and demonstrates that the main mechanism of dye removal from the contact solution is caused by adsorption onto P25.

In the presence of CDCA during the dye uptake, the TGA profile shows a higher weight loss and a slight shift of all the degradation processes to lower temperatures. A shift of the onset of the degradation process (which appears above 200 °C) is anticipated of ≈ 20 °C with respect to the D5-P25 system (observed at 220 °C), and the maximum of the degradation rate is anticipated of ≈ 9 °C. Compared with D5-sensitized P25, the additional weight difference (0.68%) suggests the presence of CDCA cogenerated with D5 in the sample. An approximate 1:10 ratio between CDCA and D5 on the TiO₂ surface can be estimated from this experiment.

D5 sorption on commercial TiO₂ slides

After the successful experiment on P25 powders, an analogous FFD 2³ plan was performed on commercial TiO₂ slides to investigate the principal and the interaction effects of the three variables under real working conditions. Each experiment consisted of a sorption test in which the TiO₂ slides were immersed in 10.0 mL of a solution that contained D5 and CDCA at different concentrations for the contact times required by the experimental plan. Three replicates of the central experiment (experiments 9–11) were performed at the beginning, in the middle, and at the end of the FFD to confirm the repeatability of the analysis and to estimate the experimental error. The eight required experiments (experiments 1–8) plus three repetitions of the central point are reported in Table 6, in which uptake is ex-

Table 6. Experimental data from 2³ FFD on TiO₂-covered slides

Experiment	t	D5	CDCA	t [h]	Concentration [mmol L ^{−1}]		D5 uptake [10 ¹⁹ molec cm ^{−3}]
					D5	CDCA	
1	−	−	−	8.0	0.05	0.0	4.0
2	+	−	−	24.0	0.05	0.0	3.5
3	−	+	−	8.0	0.50	0.0	56.3
4	+	+	−	24.0	0.50	0.0	35.7
5	−	−	+	8.0	0.05	16.0	5.3
6	+	−	+	24.0	0.05	16.0	6.3
7	−	+	+	8.0	0.50	16.0	51.3
8	+	+	+	24.0	0.50	16.0	60.8
9	0	0	0	16.0	0.27	8.0	29.1
10	0	0	0	16.0	0.27	8.0	28.9
11	0	0	0	16.0	0.27	8.0	29.2

pressed, different from experiments with TiO₂ powders in which the number of molecules taken up in a unit volume of TiO₂ [molec cm^{−3}] is given. This unit was chosen because is more direct from a technological application viewpoint and because an accurate evaluation of the weight of TiO₂ film on slides is impossible. Uptake values in this unit can be calculated if we know the thickness of the slides (6.5 ± 0.4 μm), which is homogeneous within the experimental error (Experimental Section). This homogeneity allows us to compare data from different slides and to transform the amount of grafted molecules from molec cm^{−2} of a slide (the quantity used for technological applications) to molec cm^{−3} of TiO₂ (used in the TiO₂ slide experiments) and molec mg^{−1} of TiO₂ used in the powder experiments. Notably, the large apparent differences in the data presented in Tables 4 and 6 (three orders of magnitude) is because of the different measurement units.

From these results, the following OLS model was obtained for D5 uptake by TiO₂ slides (10¹⁹ molec cm^{−3}), that is, Y_s in Equation (2):

$$Y_s = 28.2 + 23.1 D5 + 3.0 CDCA + 3.96 t CDCA + 2.0 D5 - CDCA + 3.6 t D5 CDCA \quad (2)$$

This yielded satisfactory results ($R^2=0.9850$), and the observed and predicted values are in good agreement (Figure S5B).

D5 and CDCA are the only principal relevant factors and are both associated with a positive effect, contrary to TiO_2 powder FFD [Eq. (1)] in which CDCA has a negative effect. Moreover, the interactions of two and three factors are relevant. In this case, the information contained in the three-factor interaction can be extracted efficiently and shown by a graphical method that considers the three possible two-way tables constructed from the variation of the experimental response if a couple of factors is varied each time and the third factor is constant.

From the data shown in Table 7, it is clear that if the D5 concentration is high (left), it is possible to obtain a large D5 uptake in many different situations (i.e., at short contact times

Table 7. Two-way table that illustrates the D5*CDCA*t three-factor interaction: here only the table obtained for D5 fixed at high and low values is presented, the other two tables (for fixed values of CDCA and t) are shown in Figure S7.

		D5 uptake [10^{19} molec cm^{-3}]			
		at high values		at low values	
CDCA concentration [mmol L^{-1}]	16.0	51.3	60.8	5.3	6.3
	0.0	56.3	35.7	4.	3.5
		8.0	24.0	8.0	24.0
		t [h]			

in the absence of CDCA, 56.3×10^{19} molec cm^{-3} , or even in the presence of a high concentration CDCA if the contact time is long, 60.8×10^{19} molec cm^{-3}). This behavior is caused by the polydispersity of the TiO_2 substrate, which presents a distribution of adsorption sites. At shorter times and without CDCA, kinetic effects prevail and less stable, more accessible sites are saturated. Conversely, at longer times thermodynamic equilibrium is reached, which saturates stable sites with a partial bleaching of less stable sites.

At low values of D5 (Table 7, right) the best result was obtained if the values of the concentration of CDCA and t are high, but the grafted amounts are very small and comparable to the experimental error, so the recorded variations cannot be considered as statistically significant; the same considerations can be taken into account for the other two-way tables (Figure S7). In addition, the evaluation of the second-order effect, with the addition of further variable levels to be investigated, was not required as the result of the F test for the presence of the quadratic effect was negative.^[42]

The higher uptake conditions in the most interesting cases of high D5 concentrations can also be seen clearly in Figure 5, which provides a 3D visualization of the data shown in Table 7.

The different effect of the concentration of CDCA on TiO_2 slides and powder can be explained by the different diffusion conditions and available space for the D5 molecules in the two samples. In the powder sample, the TiO_2 nanoparticles are suspended in the solvent with no diffusion limitations and are

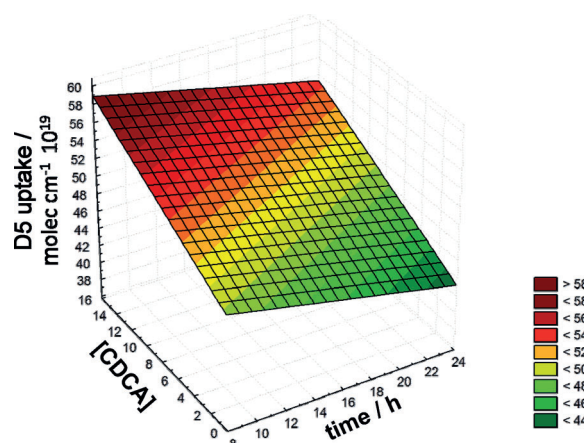


Figure 5. Surface plot that illustrates the D5*CDCA*t three-factor interaction obtained for D5 at fixed high concentration constructed from the two-way tables. The other two interactions (for fixed values of CDCA concentration and t) are shown in Figure S7.

easily accessible to D5. At the same time, at a concentration of the order of 10^{-4} M, D5 molecules are diluted, and aggregation effects are limited either in the presence or in absence of CDCA. On the contrary, on slide samples, if D5 molecules approach the TiO_2 slide surface and start to penetrate into the interstitial space among the nanoparticles of the TiO_2 layer, the available space is much smaller, and diffusion becomes a limiting step with a compromise between kinetic and thermodynamic effects (as discussed with respect to the data shown in Table 7). D5 molecules are then constrained close to each other, which thus facilitates the formation of dimers and aggregates induced by the interactions unraveled by XRD and calculations. In this situation, the action of CDCA as a dispersant becomes important to optimize the dye uptake, especially at high concentrations and for long soaking times, as both factors are able to induce aggregation. An understanding the driving forces of the aggregation processes by analysis of the structural and molecular interactions is then of paramount importance for the interpretation of the dye-uptake results, which is summarized in the following section.

Discussion of the combined approach

The structures obtained from XRD show the most stable conformations suggested by the calculations on the isolated molecules. This implies that the intermolecular interactions that dictate the crystal packing are not strong enough to vary the thermodynamically stable conformations. Several weak interactions, besides the expected H bonds, were observed in the three structures, all of which showed close contacts between the phenyl moieties. The D5 precursor **4** showed T-shaped interactions between thiophene groups, whereas D5 showed parallel packing of the aromatic moieties. These two kinds of stacking are also probable on the TiO_2 surface with no definite preference for either arrangement. It can be inferred that the same interactions must play an important role and induce aggregation of D5-related molecules in solution and on the TiO_2

surface. These aggregation forces can explain the well-known dispersion problems shown by D5 and by D5 on TiO₂ surfaces, that is, self absorption and lateral charge transfer between different dye molecules, with reduction of the injection yields.

The information on the energy barriers suggests that preparation and soaking conditions allow the coexistence (in solution and on the surface) of a variety of conformers that are different from the most stable ones. Moreover, the electron injection yield during DSC function can be conformer-dependent in principle, as different conformations show different planarity and the electronic conjugation along the D5 framework is modified. A computational study of the excited state structures, which takes into account both flexibility and conformational freedom, might provide more insight into the “real world”.

XRD analysis and calculations gave interesting indications of the structure of D5 in different situations but could not evaluate the importance of the dispersant (CDCA) and the influence of the soaking time, concentration of reagents, and the physical form of TiO₂ (powder or slide) on the dye-uptake mechanism. The spectroscopy measurements, aided by a chemometric approach to reduce the number of experiments and investigate the interactions between the various parameters that influence dye uptake, allowed us to look into some of the issues in which XRD could not provide an insight.

The FFD indicated, initially, that TiO₂ powder and slides behave differently (the role of CDCA is relevant only on TiO₂ slides; Table 7), likely because of the greater importance of diffusion problems in the solid sintered thin film. Therefore, of the studied models, the reference model must comprise TiO₂ slides. In this case, time and CDCA concentration are antagonists, therefore, the presence of CDCA allows a large dye uptake only with long soaking times, whereas good uptakes can be obtained at short soaking times without CDCA. These two situations both allow large uptakes, but with long soaking times in the presence of CDCA a uniform sparse TiO₂ loading is obtained, as suggested by the high injection yields,^[7,14] whereas with a short soaking time and no CDCA, D5 aggregation and island formation probably occurs on the TiO₂ surface.

Conclusions

First-principles calculations, XRD, UV/Vis spectroscopy, thermogravimetric analysis (TGA), and design of experiment (DoE) techniques have been used in a synergic way to shed light on the destiny of dye molecules before, during, and after the grafting process on TiO₂ electrodes. Key components of dye-sensitized solar cells (DSC), that is, dye and TiO₂, have been studied from the viewpoints of the molecular structure and of the dye-uptake mechanism using the well-known D5 molecule as a case study. This combined characterization approach provided detailed information on the molecular interactions, stable conformations, and flexibility of the dye molecules. Relaxed potential energy scan calculations, in addition to facilitating structure solutions by powder XRD, suggested that dyes can exploit their conformational flexibility to optimize grafting and packing on the TiO₂ surface with a wider than expected

available conformational landscape. These data are fundamental for us to better understand the role of chenodeoxycholic acid (CDCA) and the optimized uptake conditions of D5 on a TiO₂ slides under working conditions. The ability of CDCA to modify dye uptake (DoE), that is, that to hinder phenyl–phenyl intermolecular contact and contrast the T-shaped and parallel stacking (XRD) by intercalating on TiO₂ (TGA) between adjacent D5 molecules, is clarified by the quantitative measurement (UV/Vis) of the parameters involved in dye uptake.

The DoE-assisted spectroscopic investigation was applied to evaluate the dye uptake in DSC. The successful interpretation of the obtained model, performed by complementary characterization techniques, allowed us to propose the presented UV/Vis–DoE approach as the simplest, fastest, most reproducible, and sensitive method that can be applied widely to understand and optimize the uptake of any kind of dye.

Experimental Section

Materials

TiO₂ (Degussa P25, purity 99.5%; Germany), ethanol (purity 99.8%), and CDCA (>97%) were purchased from Sigma–Aldrich (Milwaukee, WI, USA). Glass slides covered with TiO₂ were purchased from DyeSol Italia (Rome, Italy). The D5 stock solution was prepared at 5.0×10^{-4} M by dissolving 0.0445 g of D5 in 200.0 mL of ethanol; working solutions at different concentrations were obtained by dilution of the stock solution with ethanol.

Synthesis

Full details on the synthesis of **3**, **4**, D5, and **6** are available in Section S1 in the Supporting Information.

Instrumentation

¹H and ¹³C NMR spectra were recorded by using an Avance-200 instrument (Bruker, Milan, Italy) at 200 and 50 MHz, respectively. ESI-MS spectra were recorded by using a LCQ Deca XP plus spectrometer (ThermoElectron Corporation, Rodano, MI, Italy) as detailed in the Supporting Information (Section S1). UV/Vis data were collected by using a UV/Vis Lambda 900 spectrophotometer (PerkinElmer, Monza, MI, Italy). TGA measurements were performed by using a TGA/DTA LF1100/851e instrument equipped with Store Software (Mettler Toledo, Novate Milanese, MI, Italy) under the following standard conditions: equilibration step at 60 °C for 30 min followed by a ramp at 10 °C min⁻¹ rate up to 800 °C. Measurements were collected under an air flow. XRPD measurements to analyze TiO₂ particle size were performed by using a ThermoARL powder diffractometer XTRA, and the details are given in the Supporting Information.

Single-crystal diffraction data were collected by using an Oxford Xcalibur CCD area detector diffractometer with graphite monochromator and MoK_α ($\lambda = 0.71069$ Å) radiation. Data reduction and absorption corrections were performed using CrysAlisPRO 171.34.44 (Agilent Technologies, Cernusco, MI, Italy). Single-crystal structure solution was performed by direct methods using SIR2011^[43] and refinement with full-matrix least-squares employing SHELX-97^[44]. H atoms were generated in calculated positions by SHELX-97. Single crystals of **4** and **6** suitable for X-ray analysis were

obtained by the slow cooling of a saturated hot ethanol solution. Attempts to grow D5 crystals from different solvents and different temperature conditions only yielded small micron-sized crystals, and an XRPD experiment had to be performed instead using the microcrystals grown in acetonitrile. Relevant crystal data are reported in the Supporting Information. XRPD experiments were performed at the ESRF in Grenoble on the BM1A and BM1B beamlines by using a high-resolution powder diffraction instrument (for indexing) and a Pilatus 2M detector^[45] placed at a distance of 120 cm at two different heights with respect to the incoming X-ray beam to obtain a low and high 2θ angular range (used for structure solution). The Pilatus XRPD patterns were collected by using radiation with $\lambda = 0.7040(1)$ Å. The calibration was performed using the lattice parameters of the NIST lanthanum hexaboride (LaB_6) standard (SRM 660b; nominal $a = 4.15695(6)$ Å at RT). The crystal structure was solved from XRPD data by simulated annealing using the low-angle dataset only by EXPO2011 software.^[46] The two powder patterns, at low and high 2θ range, were refined together by the Rietveld method using TOPAS software.^[47] Full details of the crystallographic measurements are reported in the Supporting Information.

Theoretical calculations

The structural models of D5 were obtained by first-principles DFT calculations employing G03^[48] software. A careful analysis of stable energy minima and of the energy barriers that separate them was performed by using the B3LYP^[49] functional and different basis sets.

Determination of D5 uptake

Sorption experiments were performed by adding, under static conditions, appropriate amounts of D5 to the selected amounts of P25 powder for each experiment. The systems were stirred magnetically for 16 h; then a portion of the solution (1.00 mL) was collected, which was centrifuged twice at 26 °C and 3000 rpm for 15.0 min and filtered through a 0.20 μm polypropylene membrane (VWR International, West Chester, PA, USA). UV/Vis analysis was performed at 447.9 nm for the determination of the amount of dye still present in solution. All solutions were maintained in the dark.

The particle size and film thickness of the transparent TiO_2 -covered glass (TiO_2 slides), purchased from Dyesol, were characterized by XRPD and UV/Vis-NIR spectroscopy, respectively (Figures S1 and S2). A particle size of ≈ 25 nm and a thickness of the TiO_2 film of (6.5 ± 4) μm were determined. These values were used to calculate the amount of available grafting sites and to estimate the amount of D5 that can be adsorbed by a single slide for a better design of the preliminary experimental plan. The TiO_2 thickness was confirmed by NIR spectroscopy (Figure S2 and Table S1) by analysis of the absorption interference fringes of the TiO_2 slides, generated by the similarity of the radiation wavelength and the TiO_2 thickness.^[50]

The transparent TiO_2 slides were immersed under static conditions in a beaker in different solutions (10.00 mL) that contained different amounts of D5 and CDCA for the contact times dictated by the DoE. Usually, concentrations and contact times are optimized by trial and error. Typical literature^[7–14] conditions are 1–0.1 mM for D5, 10 mM for CDCA, and 16 h contact time (overnight). Their values were chosen for the DoE to explore the variable space and find the optimal soaking conditions.

The solution was collected, filtered, and analyzed by UV/Vis spectroscopy (447.9 nm) to determine the amount of dye still present in solution. All the solutions were maintained in the dark.

After the sorption experiments, the P25 powder and TiO_2 slides were washed with ethanol (2×10.00 mL); the aliquots were then recovered, centrifuged, filtered, and analyzed by UV/Vis spectroscopy under the same conditions of the sorption experiments.

Chemometric analysis

FFD, regression models, and all graphical representations were performed by using Statistica 7.1 (Statsoft Inc., USA) and Excel 2013 (Microsoft Corporation, USA).

Acknowledgements

We would like to thank A. Coelho (Coelho Software Brisbane, Australia) for his advice and especially for the use of constraints in the TOPAS program. Prof. Davide Viterbo is acknowledged for useful suggestions and discussion during data analysis and manuscript preparation. ESRF and SNBL are acknowledged for beam time. D. Chernyshov (SNBL, Grenoble, FR) is acknowledged for support in data collection and reduction of XRPD Pilatus 2M data. Fondazione CRC (grant n. 2008–1581) is gratefully acknowledged for funding. L.P. acknowledges financial contributions from the MIUR project “Multidisciplinary modeling of the structure of layered materials” funded as FIRB in 2012, (code RBFR10CWDA) for funding his bursary. C.B. and V.G. gratefully acknowledge financial support by DSSCX project (PRIN 2010–2011, 20104XET32) from Ministero dell’Istruzione, dell’Università e della Ricerca. Finally, G.F. thanks the “Scuola di Alta Formazione” of the University of Piemonte Orientale (Italy) and Compagnia di San Paolo for funding her PhD bursary.

Keywords: density functional calculations • dyes/pigments • titanium • UV/Vis spectroscopy • X-ray diffraction

- [1] a) M. Grätzel, *Acc. Chem. Res.* **2009**, *42*, 1788–1798; b) A. Hagfeldt, G. Boschloo, L. Sun, L. Kloo, H. Pettersson, *Chem. Rev.* **2010**, *110*, 6595–6663; c) J. Burschka, N. Pellet, S. J. Moon, R. Humphry-Baker, P. Gao, M. K. Nazeeruddin, M. Grätzel, *Nature* **2013**, *499*, 316–319.
- [2] H. S. Jung, J. K. Lee, *J. Phys. Chem. Lett.* **2013**, *4*, 1682–1693.
- [3] R. Y. Ogura, S. Nakane, M. Morooka, M. Orihashi, Y. Suzuki, K. Noda, *APL* **2009**, 073308.
- [4] For comprehensive reviews, see: a) H. Imahori, T. Umeyama, S. Ito, *Acc. Chem. Res.* **2009**, *42*, 1809–1818; b) A. Mishra, M. K. R. Fischer, P. Bauerle, *Angew. Chem. Int. Ed.* **2009**, *48*, 2474–2499; *Angew. Chem.* **2009**, *121*, 2510–2536; c) J. N. Clifford, M. Planells, E. Palomares, *J. Mater. Chem.* **2012**, *22*, 24195–24201; d) J. Park, G. Viscardi, C. Barolo, N. Barbero, *Chimia* **2013**, *67*, 129–135; for some selected recent examples, see: e) A. Yella, H.-W. Lee, H. N. Tsao, C. Yi, A. K. Chandiran, M. K. Nazeeruddin, E. W.-G. Diao, C. Y. Yeh, S. M. Zakeeruddin, M. Grätzel, *Science* **2011**, *334*, 629–634; f) J. Park, C. Barolo, F. Sauvage, N. Barbero, C. Benzi, P. Quagliotto, S. Coluccia, D. Di Censo, M. Grätzel, M. K. Nazeeruddin, G. Viscardi, *Chem. Commun.* **2012**, *48*, 2782–2784; g) C. Barolo, J.-H. Yum, E. Artuso, N. Barbero, D. Di Censo, M. G. Lobello, S. Fantacci, F. De Angelis, M. Grätzel, M. K. Nazeeruddin, G. Viscardi, *ChemSusChem* **2013**, *6*, 2170–2180.
- [5] N. Cai, R. Li, Y. Wang, M. Zhang, P. Wang, *Energy Environ. Sci.* **2013**, *6*, 139–147.

- [6] a) B. O'Regan, L. Xiao, T. Ghaddar, *Energy Environ. Sci.* **2012**, *5*, 7203–7215; b) V. Johansson, L. Ellis-Gibbings, T. Clarke, M. Gorlov, G. G. Andersson, L. Kloo, *Phys. Chem. Chem. Phys.* **2014**, *16*, 711–718.
- [7] D. P. Hagberg, J.-H. Yum, H. J. Lee, F. De Angelis, T. Marinado, K. M. Karlsson, R. Humphry-Baker, L. Sun, A. Hagfeldt, M. Grätzel, Md. K. Nazeeruddin, *J. Am. Chem. Soc.* **2008**, *130*, 6259–6266.
- [8] E. Ronca, M. Pastore, L. Belpassi, F. Tarantelli, F. De Angelis, *Energy Environ. Sci.* **2013**, *6*, 183–193.
- [9] M. Pastore, E. Mosconi, F. De Angelis, M. Grätzel, *J. Phys. Chem. C* **2010**, *114*, 7205–7212.
- [10] F. Labat, T. Le Bahers, I. Ciofini, C. Adamo, *Acc. Chem. Res.* **2012**, *45*, 1268–1277.
- [11] E. Dell'Orto, L. Raimondo, A. Sassella, A. Abboto, *J. Mater. Chem.* **2012**, *22*, 11364–11369.
- [12] H.-P. Lu, C.-Y. Tsai, W.-N. Yen, C.-P. Hsieh, C.-W. Lee, C.-Y. Yeh, E. W.-G. Diau, *J. Phys. Chem.* **2009**, *113*, 20990–20997.
- [13] J. Li, W. J. Wu, J. B. Yang, J. Tang, Y. T. Long, J. L. Hua, *Science China Chem.* **2011**, *54*, 699–706.
- [14] D. P. Hagberg, T. Edvinsson, T. Marinado, G. Boshloo, A. Hagfeldt, L. Sun, *Chem. Commun.* **2006**, 2245–2247.
- [15] G. Boschloo, T. Marinado, K. Nonomura, T. Edvinsson, A. G. Agrios, D. P. Hagberg, L. Sun, M. Quintana, C. S. Karthikeyan, M. Thelakkat, A. Hagfeldt, *Thin Solid Films* **2008**, *516*, 7214–7217.
- [16] a) W. Zeng, Y. Cao, Y. Bai, Y. Wang, Y. Shi, M. Zhang, F. Wang, C. Pan, P. Wang, *Chem. Mater.* **2010**, *22*, 1915–1925; b) H. N. Tsao, J. Burschka, C. Yi, F. Kessler, M. K. Nazeeruddin, M. Grätzel, *Energy Environ. Sci.* **2011**, *4*, 4921–4924; c) H. N. Tsao, C. Yi, T. Moehl, J.-H. Yum, S. M. Zakeeruddin, M. K. Nazeeruddin, M. Grätzel, *ChemSusChem* **2011**, *4*, 591–594; d) M. Xu, M. Zhang, M. Pastore, R. Li, F. De Angelis, P. Wang, *Chem. Sci.* **2012**, *3*, 976–983.
- [17] R. Gobetto, C. Nervi, B. Romanin, L. Salassa, M. Milanese, G. Croce, *Organometallics* **2003**, *22*, 4012–4019.
- [18] A. Arrais, E. Diana, R. Gobetto, M. Milanese, D. Viterbo, P. L. Stanghellini, *Eur. J. Inorg. Chem.* **2003**, 1186–1192.
- [19] A. Arrais, E. Boccaleri, G. Croce, M. Milanese, R. Orlando, E. Diana, *CrytEngComm* **2003**, *5*, 388–394.
- [20] R. Gobetto, G. Caputo, C. Garino, S. Ghiani, C. Nervi, L. Salassa, E. Rosenberg, J. B. A. Ross, G. Viscardi, G. Martra, I. Miletto, M. Milanese, *Eur. J. Inorg. Chem.* **2006**, 2839–2849.
- [21] F. H. Allen, *Acta Crystallogr. Sect. B* **2002**, *58*, 380–388.
- [22] a) S. P. Anthony, C. Delaney, S. Varughese, L. Wang, S. M. Draper, *CrytEngComm* **2011**, *13*, 6706–6711; b) S. P. Anthony, S. Varughese, S. M. Draper, *Chem. Commun.* **2009**, 7500–7502; c) S. P. Anthony, S. Varughese, S. M. Draper, *J. Phys. Org. Chem.* **2010**, *23*, 1074–1079.
- [23] a) Y.-T. Li, C.-L. Chen, Y.-Y. Hs, H.-C. Hsu, Y. Chi, B.-S. Chen, W.-H. Liu, C.-H. Lai, T.-Y. Lin, P.-T. Chou, *Tetrahedron* **2010**, *66*, 4223–4234; b) S. Zheng, S. Barlow, C. Risko, T. L. Kinnibrugh, V. N. Khrustalev, S. C. Jones, M. Yu. Antipin, N. M. Tucker, T. V. Timofeeva, V. Coropceanu, J.-L. Bredas, S. R. Marder, *J. Am. Chem. Soc.* **2006**, *128*, 1812–1817; c) F.-R. Dai, W.-J. Wu, Q.-W. Wang, H. Tian, W.-Y. Wong, *Dalton Trans.* **2011**, *40*, 2314–2323.
- [24] E. M. J. Johansson, T. Edvinsson, M. Odelius, D. P. Hagberg, L. Sun, A. Hagfeldt, H. Siegbahn, H. Rensmo, *J. Phys. Chem. C* **2007**, *111*, 8580–8586.
- [25] G. E. P. Box, W. G. Hunter, J. S. Hunter, *Statistics for Experimenters*, Wiley, New York, **1978**.
- [26] R. Carlson, *Design and Optimisation in Organic Synthesis*, Elsevier, Amsterdam, **1992**.
- [27] S. N. Deming, S. L. Morgan, *Experimental Design: A Chemometric Approach*, Elsevier, Amsterdam, London, New York, Tokyo, **1993**.
- [28] a) F. Bella, D. Pugliese, J. R. Nair, A. Sacco, S. Bianco, C. Gerbaldi, C. Barolo, R. Bongiovanni, *Phys. Chem. Chem. Phys.* **2013**, *15*, 3706–3711; b) D. Pugliese, F. Bella, V. Cauda, A. Lamberti, A. Sacco, E. Tresso, S. Bianco, *ACS Appl. Mater. Interfaces* **2013**, *5*, 11288–11295.
- [29] Y. J. Cheng, J. Luo, S. Hau, D. H. Bale, T.-D. Kim, Z. Shi, D.-B. Lao, N. M. Tucker, Y. Tian, L. R. Dalton, P. J. Reid, A. K. Y. Jen, *Chem. Mater.* **2007**, *19*, 1154–1163.
- [30] H. Xia, J. He, B. Xu, S. Wen, Y. Li, W. Tian, *Tetrahedron* **2008**, *64*, 5736–5742.
- [31] L. J. Gooßen, J. Paetzol, L. Winkel, *Synlett* **2002**, *10*, 1721–1723.
- [32] J. W. Hagemann in *Crystallization and Polymorphism of Fats and Fatty Acids* (Eds.: N. Garti, K. Sato), Marcel Dekker Inc, New York and Basel, **1988**, pp. 9–96.
- [33] M. P. Balanay, S.-M. Kim, M. J. Lee, S. H. Lee, D. H. Kim, *Bull. Korean Chem. Soc.* **2009**, *30*, 2077–2082.
- [34] L. Palin, C. Barolo, D. Chernyshov, D. Viterbo, A. G. Moliterni, G. Croce, W. van Beek, M. Milanese, Data collection and analysis strategies for structure solution of complex organic structures, in preparation for submission to *J. Appl. Cryst.*
- [35] M. Milanese, P. Ugliengo, D. Viterbo, G. Appendino, *J. Med. Chem.* **1999**, *42*, 291–299.
- [36] The crystal structures of D5, **4**, and **6** were submitted to the CCDC data centre with submission codes CCDC 953631, 895122, and 895123, respectively. These data can be obtained free of charge from The Cambridge Crystallographic Data Centre via www.ccdc.cam.ac.uk/data_request/cif.
- [37] DoE is based on model systems of different complexity to evaluate and control the investigated variables in the appropriate variation ranges. Generally, the exploration of the experimental domain starts with a two-level FFD, which allows the effects of the principal factors and of their interactions on the investigated response to be studied. The number of experiments required is 2^p , in which p is the number of investigated factors. These experiments correspond to all the possible combinations of the two levels (usually indicated by + and –) of the considered factors; then, if necessary, other experiments are added to study the second-order effects of the investigated factors.
- [38] V. Gianotti, M. Benzi, G. Croce, P. Frascarolo, F. Gosetti, E. Mazzucco, M. Bottaro, M. C. Gennaro, *Chemosphere* **2008**, *73*, 1731–1736.
- [39] S. Polati, F. Gosetti, V. Gianotti, M. C. Gennaro, *J. Environ. Sci. Health Part B* **2006**, *41*, 765–779.
- [40] a) P. Ugliengo, D. Viterbo, G. Chiari, Z. Kristallogr. **1993**, *207*, 9–23; b) <http://www.moldraw.unito.it>.
- [41] To verify if the D5 molecules were grafted effectively on the P25 powder, two washing procedures were tested. In the first, the P25 powder that remained after centrifugation in experiments 6 and 7 was contacted with 10.0 mL ethanol and left to stand overnight. The solution was centrifuged (3000 rpm, 26 °C, 15 min), and the powder was again contacted with 10.0 mL ethanol for 10 min. The solution was centrifuged, and the supernatant was combined with that obtained from the first centrifugation and analyzed by UV/Vis. The second method differed only in the contact time of the first ethanol aliquot, which was 10 min. The number of molecules removed by the two treatments was similar and of approximately the same order of magnitude as the estimated standard deviation, which indicates that the molecules of D5 are tightly bonded to the surface of TiO₂ and not only physisorbed and/or stacked on the surface in weakly bound multilayers.
- [42] A. I. Khuri, J. A. Cornell, *Response Surface, Design and Analysis*, Marcel Dekker, New York, **1987**.
- [43] M. C. Burla, R. Caliendo, M. Camalli, G. L. Cascarano, C. Giacovazzo, M. Mallamo, A. Mazzone, G. Polidori, R. Spagna, *J. Appl. Crystallogr.* **2012**, *45*, 357–361.
- [44] G. M. Sheldrick, *Acta Crystallogr. Sect. A* **2008**, *64*, 112–122.
- [45] B. Henrich, A. Bergamaschi, C. Broennimann, R. Dinapoli, E. F. Eikenberry, I. Johnson, M. Kobas, P. Kraft, A. Mozzanica, B. Schmitt, *Nucl. Instrum. Methods Phys. Res. Sect. A* **2009**, *607*, 247–249.
- [46] a) EXPO2011, version 1.12.09a, <http://www.ba.cnr.it>; b) A. Altomare, M. C. Burla, G. Cascarano, C. Giacovazzo, A. Guagliardi, A. G. G. Moliterni, G. Polidori, *J. Appl. Crystallogr.* **1995**, *28*, 842–846; c) A. Altomare, G. Cascarano, C. Giacovazzo, A. Guagliardi, M. C. Burla, G. Polidori, M. Camalli, *J. Appl. Crystallogr.* **1994**, *27*, 435–436.
- [47] A. A. Coelho, *J. Appl. Crystallogr.* **2005**, *38*, 455–461; A. A. Coelho, *J. Appl. Crystallogr.* **2003**, *36*, 86–95.
- [48] Gaussian 03, Revision C.02, M. J. Frisch, G. W. Trucks, H. B. Schlegel, G. E. Scuseria, M. A. Robb, J. R. Cheeseman, J. A. Montgomery Jr., T. Vreven, K. N. Kudin, J. C. Burant, J. M. Millam, S. S. Iyengar, J. Tomasi, V. Barone, B. Mennucci, M. Cossi, G. Scalmani, N. Rega, G. A. Petersson, H. Nakatsuji, M. Hada, M. Ehara, K. Toyota, R. Fukuda, J. Hasegawa, M. Ishida, T. Nakajima, Y. Honda, O. Kitao, H. Nakai, M. Klene, X. Li, J. E. Knox, H. P. Hratchian, J. B. Cross, V. Bakken, C. Adamo, J. Jaramillo, R. Gomperts, R. E. Stratmann, O. Yazyev, A. J. Austin, R. Cammi, C. Pomelli, J. W. Ochterski, P. Y. Ayala, K. Morokuma, G. A. Voth, P. Salvador, J. J. Dan-

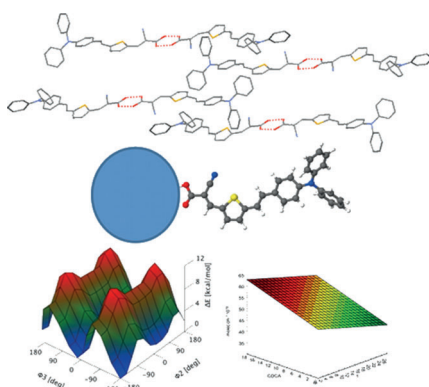
- nenberg, V. G. Zakrzewski, S. Dapprich, A. D. Daniels, M. C. Strain, O. Farkas, D. K. Malick, A. D. Rabuck, K. Raghavachari, J. B. Foresman, J. V. Ortiz, Q. Cui, A. G. Baboul, S. Clifford, J. Cioslowski, B. B. Stefanov, G. Liu, A. Liashenko, P. Piskorz, I. Komaromi, R. L. Martin, D. J. Fox, T. Keith, M. A. Al-Laham, C. Y. Peng, A. Nanayakkara, M. Challacombe, P. M. W. Gill, B. Johnson, W. Chen, M. W. Wong, C. Gonzalez, J. A. Pople, Gaussian, Inc., Wallingford CT, **2004**.
- [49] a) A. D. Becke, *J. Chem. Phys.* **1993**, *98*, 5648–5652; b) C. Lee, W. Yang, R. G. Parr, *Phys. Rev. B* **1988**, *37*, 785–789.
- [50] a) M. Caglar, Y. Caglar, S. Ilcan, *J. Optoelectr. Adv. Mater.* **2006**, *8*, 1410–1413; b) S. Ilcan, M. Caglar, Y. Caglar, *Mater. Sci. Poland* **2007**, *25*, 709–718.

Received: March 18, 2014

Published online on ■ ■ ■, 0000

FULL PAPERS

Live and let dye: A polyene-diphenylaniline dye (D5) for dye-sensitized solar cells is studied by a combination of XRD, theoretical calculations, and spectroscopic/chemometric methods. These data allow us to characterize the driving forces that govern D5 uptake and grafting, to infer the most likely arrangement of the D5 molecules on TiO_2 , and to understand the aggregation phenomena suggested by the chemometric study.



V. Gianotti, G. Favaro, L. Bonandini,
L. Palin, G. Croce, E. Boccaleri, E. Artuso,
W. van Beek, C. Barolo,* M. Milanesio*

■■■ – ■■■

**Rationalization of Dye Uptake on
Titania Slides for Dye-Sensitized Solar
Cells by a Combined Chemometric
and Structural Approach**

